Journal of. Modern Trends in Physics Research
Online ISSN 2636-4220
DOI: 10.19138/mtpr/(14)16-25
Accepted: 2014-12-19

Fine structure calculations of atomic data for Ar XVI

A. I. Refaie[1]

[1] *Physics Department, Faculty of Science, Cairo University, Giza 12613, Egypt.*

Abstract- Absolute ionization and excitation rate coefficients have been evaluated for Lithium-like Argon ion in the plasma for some arbitrary excited states at certain chosen electron temperatures kTe and for electron densities Ne. The populations of 24 excited levels are calculated for the doublet state of the Li-like Argon ion. The calculations have been carried out using the coupled rate simultaneous equations including the monopole and quadruple transitions in the calculations in addition to the dipole transitions. A theoretical population model has been developed to study the influence of the different processes, contributing to the population of the different levels on the plasma parameters. The population densities of these different levels have then been derived using these rate coefficients. Neither experimental nor theoretical data have been found in literature for comparison.

Correspondence Author – A. I. Refaie (amal1_ibrahim1@yahoo.com)

Keywords- Ionization rate coefficients; excitation rate coefficients; Lithium-Like Argon.

1. INTRODUCTION

Many of the emission lines observed in laboratory and astrophysical plasmas are formed by electron-impact excitation of multiply charged atomic ions. Interpreting and modeling the observed spectra of such plasmas requires an accurate knowledge of a large number of rate coefficients. Theoretical calculations can provide the needed rate coefficients, but experimental benchmark values are needed for the comparison. The most important rate coefficients for electron collisions which are the electron-neutral ionization and the electron impact excitation have been calculated for some states. The plasma parameters of electron are significant factors for computing the rate coefficients, namely, the electron temperature (T_e) and the electron density (N_e). Further study has been made for the heavier elements like Argon [Sapirstein and Cheng (2011); Saloman (2010); Mu-Hong and Zhi-Wen (2009); Natarajan and Natarajan (2007); Nahar (2002)]. Inner-shell excitation energy and autoionization rates for Li-, Be-, B-like ions with Z = 6–54 were calculated using the 1/Z perturbation theory method. Relativistic corrections were taken into account in the frame of the Breit operators [Safronova and Shlyaptseva (1996)]. Relativistic many-body calculations of dielectronic satellite spectra created by autoionizing 1s2*l*2*l*' states in Li-like ions including the Breit interaction, is used to evaluate energy levels, radiative matrix elements and autoionization rates [Safronova *et al.* (2010)]. Relative intensities of dielectronic satellite lines, determined by radiative transition probabilities and autoionization rates, were calculated for Li-like ions with high values of n by using the perturbation theory method [Safronova *et al.*(1997)]. Effective collision strengths, for electron-impact excitation of Al^{10+} are evaluated in the close-coupling approximation using the multichannel R-matrix method [Stancalie *et al.* (2005)].

The ion Ar XVI studied in this work, is found to be the heaviest ion allowing a rapid recombination scheme to develop a VUV or soft X-ray laser.

In the present work, the absolute electron impact excitation and ionization rate coefficients of ns (n=2-5), np (n=2-5), nd (n=3-5), nf (n=4-5) and 5g, namely for doublet states, are considered for Ar XVI.

Radiative transition probabilities, for allowed and forbidden transitions including relativistic effects in Breit-Pauli approximation, have been calculated using the Cowan code [Cowan and Griffin (1976); Cowan (1981)]. These radiative transition rates have been used in the calculations of the ionization and excitation rate coefficients, i.e., the calculations have been carried out using the coupled rate simultaneous equations where the monopole and the

Journal of. Modern Trends in Physics Research
Online ISSN 2636-4220
DOI: 10.19138/mtpr/(14)16-25
Accepted: 2014-12-19

quadrupole transitions have been included in the calculations in addition to the dipole transitions. Neither experimental nor theoretical data have been found in the literature for the rate coefficients for comparison.

A theoretical population model has been developed, to study the influence of the different processes contributing to the population of the different levels for the plasma parameters. The level populations, for these 24 different levels, have then been derived from these rate coefficients for Ar XVI. The calculations have been performed at the electron temperatures equal to both fourth of the ionization potential (in eV) and also to half its value.

2. THEORY

2.1. *Rate coefficients*

The electronic $|p\rangle \longrightarrow |n\rangle$ and $|p\rangle \longrightarrow |i\rangle$ transitions in an atom are considered, where p and n are the (effective) principal quantum numbers of initial and final states $|p\rangle$ and $|n\rangle$, and $|i\rangle$ denotes the ion ground state [Vriens (1980)]. E_{pi} denotes the ionization energy while $E_{pn} = E_n - E_p$ represents the excitation energy (for $E_n > E_p$) or de-excitation energy (for $E_n < E_p$) energies. The incident electron energy and the energy transfer to the atomare given by E_e and E, respectively.

2.1.1. Ionization rate

The ionization rate coefficient is given by [Vriens (1980)]:

$$k_{pi} = \frac{9.56 \times 10^{-6} (kT_e)^{-1.5} \exp(-\varepsilon_{pi})}{\varepsilon_{pi}^{2.33} + 4.38\varepsilon_{pi}^{1.72} + 1.32\varepsilon_{pi}} \quad cm^3 S^{-1} \qquad (1)$$

where, ε_{pi} is the energy transfer ($\varepsilon_{pi} = {E_{pi}}/{kT_e}$) and kT_e is expressed in eV.

2.1.2. Excitation rate

An empirical formula representing the numerical rate coefficients for the excitation rate with energy transfer ε_{pn} is given by:

$$k_{pn} = \frac{1.6 \times 10^{-7} (kT_e)^{0.5} \exp(-\varepsilon_{pn})}{kT_e + \Gamma_{pn}} \times \left[A_{pn} \ln\left(\frac{0.3kT_e}{R} + \Delta_{pn} \right) + B_{pn} \right] \quad cm^3 S^{-1} \qquad (2)$$

where, kT_e is in eV, R (Rydberg energy) in eV and energy transfer ε_{pn} ($\varepsilon_{pn} = {E_{pn}}/{kT_e}$) .

$$\Gamma_{pn} = R \ln\left(1 + \frac{p^3 kT_e}{R}\right)\left[3 + 11\left(\frac{s}{p}\right)^2\right] \times \left(6 + 1.6ns + \frac{0.3}{s^2} + 0.8\frac{n^{1.5}}{s^{0.5}}|s - 0.6|\right)^{-1}$$

$$R = 13.595, \; p = z_{eff} \times \sqrt{{R}/{E_{pi}}}, \; n = z_{eff} \times \sqrt{{R}/{E_{ni}}}, \; s = |n - p|$$

$$A_{pn} = \left({2R}/{E_{pn}}\right) f_{pn}$$

f_{pn} being the absorption oscillator strength.

Journal of. Modern Trends in Physics Research
Online ISSN 2636-4220
DOI: 10.19138/mtpr/(14)16-25
Accepted: 2014-12-19

$$\Delta_{pn} = exp\left(-\frac{B_{pn}}{A_{pn}}\right) + \frac{0.06s^2}{np^2}$$

where $B_{pn} = \frac{4R^2}{n^3}\left(\frac{1}{E_{pn}^2} + \frac{4E_{pi}}{3E_{pn}^3} + b_p \frac{E_{pi}^2}{E_{pn}^4}\right)$, and $b_p = \frac{1.4 \ln p}{p} - \frac{0.7}{p} - \frac{0.51}{p^2} + \frac{1.16}{p^3} - \frac{0.55}{p^4}$.

2.2. *Population densities*

The level population can be calculated by solving the steady-state rate equations [Feldman *et al.* (1986); Seaton (1987)]

$$N_j\left[\sum_{i<j} A_{ji} + N_e\left(\sum_{i>j} C_{ji}^d + \sum_{i>j} C_{ji}^e\right)\right] = N_e\left(\sum_{i<j} N_i C_{ij}^e + \sum_{i>j} N_i C_{ij}^d\right) + \sum_{i>j} N_i A_{ij} \quad (3)$$

where N_j is the population of level j, A_{ji} is the spontaneous decay rate from level j to level i (transition probabilities) and C_{ji}^e is the electron collisional excitation rate coefficient. C_{ji}^d is the collisional de-excitation rate coefficient, given by [Vriens (1980)]

$$k_{pn} = \frac{1.6\times10^{-7}(kT_e)^{0.5} g_n/g_p}{kT_e + \Gamma_{np}} \times \left[A_{np}\, ln\left(\frac{0.3kT_e}{R} + \Delta_{np}\right) + B_{np}\right] \quad (4)$$

where Γ_{np} and Δ_{np} are obtained from Γ_{pn} and Δ_{pn} by interchanging p and n and where g_p and g_n are the statistical weights of level $|\,p\rangle$ and $|\,n\rangle$.

The population of the j^{th} level is obtained from the following identity:

$$N_j = \left(\frac{N_j}{N_I}\right)\left(\frac{N_I}{N_T}\right)\left(\frac{N_T}{N_e}\right) N_e \quad (5)$$

where N_I is the total number density of all the levels of the ion under consideration and N_T is the total number density of all ionization stages. Since the populations calculated from Eq. (3) are normalized such that [Feldman *et al.* (1986); Seaton (1987)]

$$\sum_{j=1}^{n}\left(\frac{N_j}{N_I}\right) = 1 \quad (6)$$

where n=24 is the number of all levels of the ion under consideration, the quantity actually obtained from the steady-state rate equation (3) is the fractional or reduced population $\frac{N_j}{N_I}$. The population densities have been calculated at different electron temperatures and various electron densities by solving a set of 24 coupled rate equations (Eq. (3)) [Feldman *et al.*, 1983; 1984; 1985; 1986; Seaton (1987)].

3. RESULTS AND DISCUSSION

Journal of. Modern Trends in Physics Research
Online ISSN 2636-4220
DOI: 10.19138/mtpr/(14)16-25
Accepted: 2014-12-19

2.2. Ionization and excitation rate coefficients

The fine structure energy levels and transition probabilities have been calculated using the Cowan code [Cowan (1981)]. The electron impact ionization and excitation rate coefficients have been evaluated for excited atomic states in Ar XVI according to Vriens [Vriens (1980)] given by Eq. (1). The calculations have been carried out using a computer program (CRMO code) [Allam] and including all the forbidden and allowed transitions necessary for calculations. Thus, the monopole and quadrupole transitions have been introduced in addition to the dipole transitions. The rate coefficients are determined for $1s^22s$ ($^2S_{1/2}$), $1s^22p$ ($^2P_{1/2}$, $^2P_{3/2}$), $1s^23s$ ($^2S_{1/2}$), $1s^23p$($^2P_{1/2}$, $^2P_{3/2}$), $1s^23d$ ($^2D_{3/2}$, $^2D_{5/2}$), $1s^24s$ ($^2S_{1/2}$), $1s^24p$ ($^2P_{1/2}$, $^2P_{3/2}$), $1s^24d$ ($^2D_{3/2}$, $^2D_{5/2}$), $1s^24f$ ($^2F_{5/2}$, $^2F_{7/2}$), $1s^25s$ ($^2S_{1/2}$), $1s^25p$ ($^2P_{1/2}$, $^2P_{3/2}$), $1s^25d$ ($^2D_{3/2}$, $^2D_{5/2}$), $1s^25f$ ($^2F_{5/2}$, $^2F_{7/2}$) and 5g ($^2G_{7/2}$, $^2G_{9/2}$) excited atomic states in Ar XVI. The calculations have been carried out at different electron temperatures (in eV).

The ionization rates for all the levels at the different temperatures are listed in table 1.

Fig. 1 shows the relation between the electron temperature (kT_e) versus ionization rates for Ar XVI ion. The curve shows the usual behavior for the ionization trend.

Fig. 2 shows that as the principal quantum number "n" decreases, the coupling between the electrons and the nucleus increases. By increasing the temperature and for n = 2 the behavior of the energy states shows saturation. This phenomenon may be explained that as the temperature is increased the electrons from these ionization states are expelled.

The excitation rate coefficients are drawn versus the electron temperature kT_e in (in eV) as shown in Fig. (3-5) for $1s^2$ ns ($^2S_{1/2}$) - $1s^2$ np ($^2P_{1/2}$) allowed transitions and for the selected forbidden transitions at $\Delta n = 0$ and 1, respectively, for Lithium-like Ar XVI ion.

Excitation rate coefficients have been calculated as a function of electron temperature by using Eq. (2).

Table 1. Electron temperature and ionization rates for ground and excited atomic states in Ar XVI.

Temperature (eV)	Ionization coefficient ($cm^3\ s^{-1}$)							
	2s $^2S_{1/2}$	2p $^2P_{1/2}$	2p $^2P_{3/2}$	3s $^2S_{1/2}$	3p $^2P_{1/2}$	3p $^2P_{3/2}$	3d $^2D_{3/2}$	3d $^2D_{5/2}$
10	7.44E-12	8.09E-12	8.16E-12	5.63E-11	5.96E-11	6.00E-11	6.13E-11	6.14E-11
20	1.19E-11	1.30E-11	1.31E-11	8.68E-11	9.18E-11	9.23E-11	9.43E-11	9.44E-11
30	1.55E-11	1.68E-11	1.70E-11	1.10E-10	1.17E-10	1.17E-10	1.20E-10	1.20E-10
40	1.86E-11	2.01E-11	2.03E-11	1.31E-10	1.38E-10	1.39E-10	1.42E-10	1.42E-10
50	2.13E-11	2.30E-11	2.32E-11	1.49E-10	1.57E-10	1.58E-10	1.62E-10	1.62E-10
100	3.20E-11	3.47E-11	3.49E-11	2.26E-10	2.40E-10	2.41E-10	2.46E-10	2.47E-10
150	4.06E-11	4.40E-11	4.43E-11	2.99E-10	3.17E-10	3.19E-10	3.26E-10	3.27E-10
200	4.82E-11	5.23E-11	5.27E-11	3.74E-10	3.99E-10	4.01E-10	4.11E-10	4.12E-10
250	5.54E-11	6.02E-11	6.07E-11	4.57E-10	4.88E-10	4.92E-10	5.04E-10	5.05E-10
300	6.25E-11	6.79E-11	6.85E-11	5.50E-10	5.89E-10	5.94E-10	6.09E-10	6.11E-10
350	6.95E-11	7.56E-11	7.63E-11	6.56E-10	7.05E-10	7.10E-10	7.30E-10	7.32E-10
400	7.66E-11	8.35E-11	8.42E-11	7.76E-10	8.37E-10	8.44E-10	8.68E-10	8.71E-10
450	8.39E-11	9.16E-11	9.24E-11	9.15E-10	9.90E-10	9.99E-10	1.03E-09	1.03E-09
500	9.14E-11	9.99E-11	1.01E-10	1.07E-09	1.17E-09	1.18E-09	1.21E-09	1.22E-09

Table 1. continue

Temperature (eV)	Ionization coefficient ($cm^3\ s^{-1}$)							
	4s $^2S_{1/2}$	4p $^2P_{1/2}$	4p $^2P_{3/2}$	4d $^2D_{3/2}$	4d $^2D_{5/2}$	4f $^2F_{5/2}$	4f $^2F_{7/2}$	5s $^2S_{1/2}$

Journal of. Modern Trends in Physics Research
Online ISSN 2636-4220
DOI: 10.19138/mtpr/(14)16-25
Accepted: 2014-12-19

10	2.75E-10	2.89E-10	2.90E-10	2.96E-10	2.96E-10	2.97E-10	2.97E-10	1.21E-09
20	4.14E-10	4.34E-10	4.36E-10	4.44E-10	4.45E-10	4.46E-10	4.46E-10	1.83E-09
30	5.25E-10	5.51E-10	5.54E-10	5.64E-10	5.65E-10	5.66E-10	5.66E-10	2.39E-09
40	6.25E-10	6.56E-10	6.59E-10	6.72E-10	6.73E-10	6.74E-10	6.75E-10	2.95E-09
50	7.20E-10	7.56E-10	7.60E-10	7.75E-10	7.76E-10	7.78E-10	7.78E-10	3.55E-09
100	1.20E-09	1.27E-09	1.28E-09	1.31E-09	1.31E-09	1.31E-09	1.31E-09	7.63E-09
150	1.79E-09	1.90E-09	1.92E-09	1.96E-09	1.97E-09	1.97E-09	1.97E-09	1.50E-08
200	2.56E-09	2.74E-09	2.76E-09	2.83E-09	2.84E-09	2.85E-09	2.85E-09	2.88E-08
250	3.60E-09	3.87E-09	3.90E-09	4.02E-09	4.03E-09	4.04E-09	4.04E-09	5.45E-08
300	5.00E-09	5.41E-09	5.46E-09	5.63E-09	5.65E-09	5.67E-09	5.67E-09	1.02E-07
350	6.90E-09	7.52E-09	7.59E-09	7.85E-09	7.87E-09	7.90E-09	7.91E-09	1.92E-07
400	9.47E-09	1.04E-08	1.05E-08	1.09E-08	1.09E-08	1.10E-08	1.10E-08	3.59E-07
450	1.30E-08	1.44E-08	1.45E-08	1.51E-08	1.51E-08	1.52E-08	1.52E-08	6.72E-07
500	1.77E-08	1.98E-08	2.00E-08	2.08E-08	2.09E-08	2.10E-08	2.10E-08	1.25E-06

Fig. 3 for the $1s^2$ ns ($^2S_{1/2}$) - $1s^2$ np ($^2P_{1/2}$) allowed radiative transitions for Ar XVI shows that the curves are divided into groups according to n, that is by increasing n, the coupling between the electrons and the nucleus becomes weaker. It can also be shown that by increasing the temperature the excitation rate coefficients are decreasing when n increases due to the fact that they are far from the nucleus. There is no data available in the literature to be compared with.

Journal of. Modern Trends in Physics Research
Online ISSN 2636-4220
DOI: 10.19138/mtpr/(14)16-25
Accepted: 2014-12-19

Table 1. continue

Temperature (eV)	Ionization coefficient ($cm^3\ s^{-1}$)							
	5p $^2P_{1/2}$	5p $^2P_{3/2}$	5d $^2D_{3/2}$	5d $^2D_{5/2}$	5f $^2F_{5/2}$	5f $^2F_{7/2}$	5g $^2G_{7/2}$	5g $^2G_{9/2}$
10	1.28E-09	1.28E-09	1.31E-09	1.31E-09	1.31E-09	1.31E-09	1.31E-09	1.31E-09
20	1.93E-09	1.94E-09	1.98E-09	1.98E-09	1.99E-09	1.99E-09	1.99E-09	1.99E-09
30	2.52E-09	2.53E-09	2.58E-09	2.59E-09	2.59E-09	2.60E-09	2.60E-09	2.60E-09
40	3.12E-09	3.14E-09	3.20E-09	3.21E-09	3.21E-09	3.22E-09	3.22E-09	3.22E-09
50	3.76E-09	3.78E-09	3.86E-09	3.87E-09	3.88E-09	3.88E-09	3.89E-09	3.89E-09
100	8.18E-09	8.25E-09	8.47E-09	8.49E-09	8.51E-09	8.52E-09	8.53E-09	8.54E-09
150	1.63E-08	1.65E-08	1.70E-08	1.71E-08	1.71E-08	1.72E-08	1.72E-08	1.72E-08
200	3.17E-08	3.21E-08	3.33E-08	3.34E-08	3.36E-08	3.36E-08	3.37E-08	3.37E-08
250	6.09E-08	6.17E-08	6.44E-08	6.47E-08	6.49E-08	6.51E-08	6.52E-08	6.52E-08
300	1.16E-07	1.18E-07	1.24E-07	1.24E-07	1.25E-07	1.25E-07	1.26E-07	1.26E-07
350	2.21E-07	2.25E-07	2.37E-07	2.39E-07	2.40E-07	2.40E-07	2.41E-07	2.41E-07
400	4.20E-07	4.27E-07	4.54E-07	4.57E-07	4.59E-07	4.60E-07	4.61E-07	4.62E-07
450	7.97E-07	8.12E-07	8.68E-07	8.73E-07	8.78E-07	8.81E-07	8.83E-07	8.85E-07
500	1.51E-06	1.54E-06	1.66E-06	1.67E-06	1.68E-06	1.69E-06	1.69E-06	1.69E-06

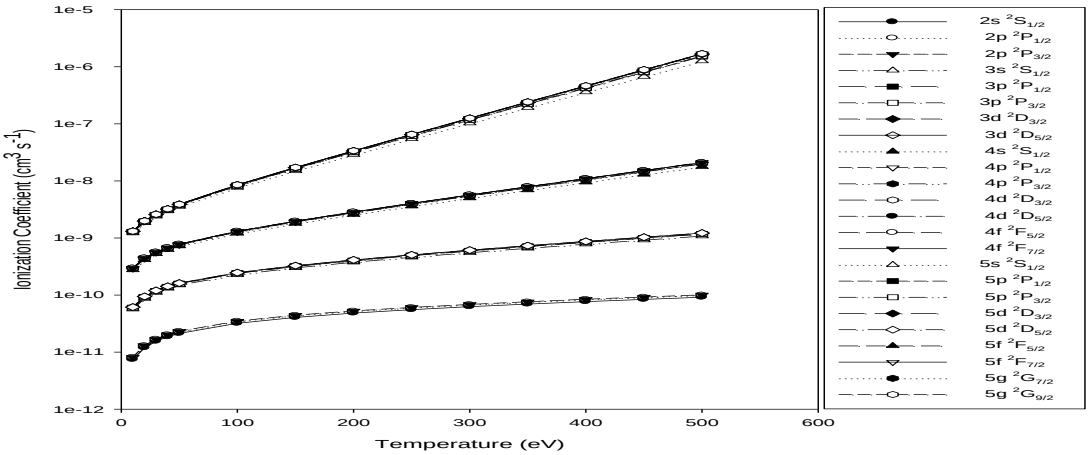

Fig. 1. Ionization rate coefficients of all levels for Ar XVI.

The ionization rates for the levels $1s^2$ ns ($^2S_{1/2}$) and $1s^2$ np ($^2P_{1/2}$), where n = 2-5 are drawn versus the electron temperature (kT_e) as shown in Fig. 2 for Ar XVI ion.

Journal of. Modern Trends in Physics Research
Online ISSN 2636-4220
DOI: 10.19138/mtpr/(14)16-25
Accepted: 2014-12-19

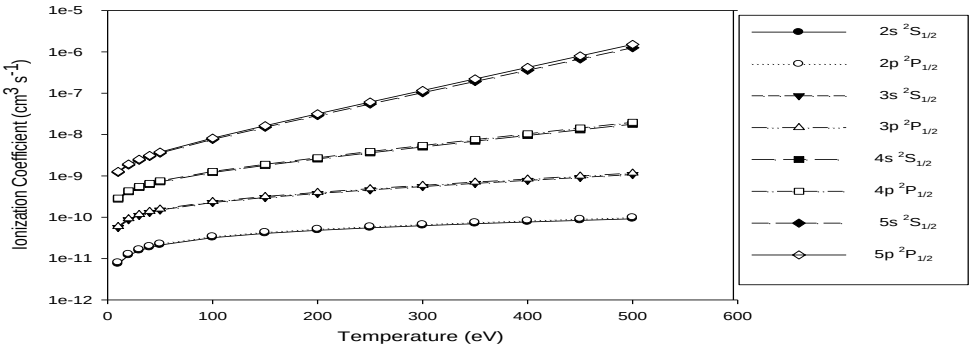

Fig. 2. Ionization rate coefficients for $1s^2$ ns ($^2S_{1/2}$) and $1s^2$ np ($^2P_{1/2}$), where (n = 2-5) for Ar XVI.

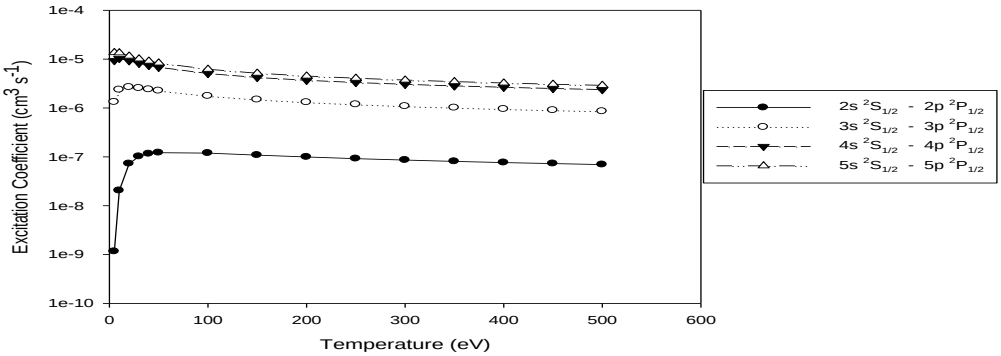

Fig. 3. Excitation rate coefficients of $1s^2$ ns ($^2S_{1/2}$) - $1s^2$ np ($^2P_{1/2}$) allowed transitions for Ar XVI.

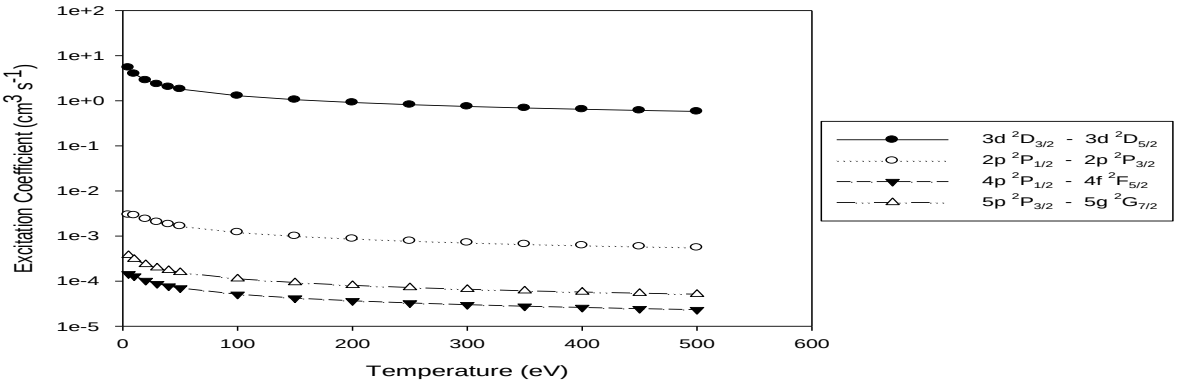

Fig. 4. Excitation rate coefficients for selected forbidden transitions at Δn=0 for Ar XVI.

Journal of. Modern Trends in Physics Research
Online ISSN 2636-4220
DOI: 10.19138/mtpr/(14)16-25
Accepted: 2014-12-19

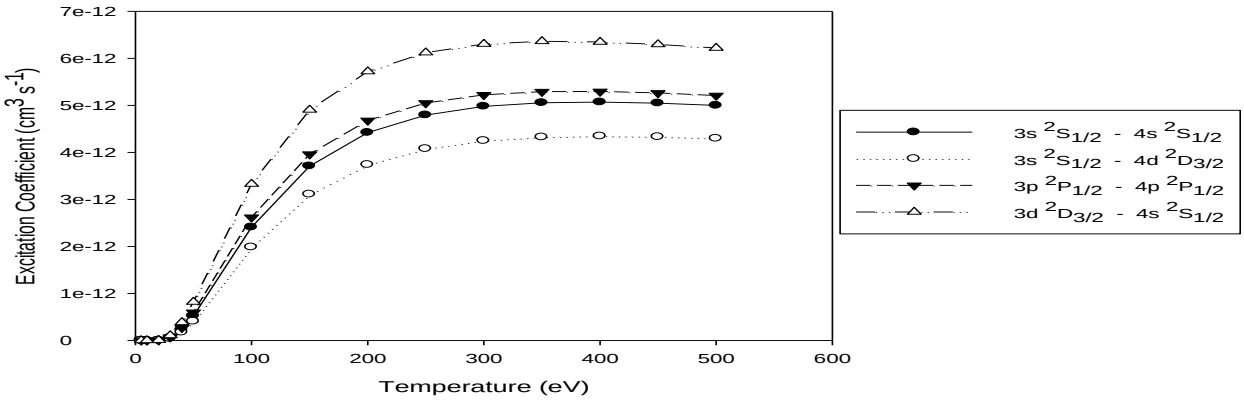

Fig. 5. Excitation rate coefficients for the selected forbidden transitions at Δn=1 for Ar XVI.

2.1. The population density of the exited levels

The level populations N_j are calculated by solving the 24 coupled rate Eq. (3) belonging to the configurations $1s^22s$ ($^2S_{1/2}$), $1s^22p$ ($^2P_{1/2}$, $^2P_{3/2}$), $1s^23s$ ($^2S_{1/2}$), $1s^23p$($^2P_{1/2}$, $^2P_{3/2}$), $1s^23d$ ($^2D_{3/2,}$ $^2D_{5/2}$), $1s^24s$ ($^2S_{1/2}$), $1s^24p$ ($^2P_{1/2}$, $^2P_{3/2}$), $1s^24d$ ($^2D_{3/2,}$ $^2D_{5/2}$), $1s^24f$ ($^2F_{5/2}$, $^2F_{7/2}$), $1s^25s$ ($^2S_{1/2}$), $1s^25p$ ($^2P_{1/2}$, $^2P_{3/2}$), $1s^25d$ ($^2D_{3/2,}$ $^2D_{5/2}$), $1s^25f$ ($^2F_{5/2}$, $^2F_{7/2}$) and $1s^25g$ ($^2G_{7/2}$, $^2G_{9/2}$) excited atomic states in Ar XVI ion. The spontaneous decay rate $A(j,i)$ given in Eq. (3) is calculated using Cowan code [Cowan and Griffin (1976); Cowan (1981)]. To calculate the population densities, the parameters C^e and C^d are substituted into the coupled rate equations. Fractional population densities are obtained using Eq. ((5) and (6)) and the CRMO code [Allam] for solving simultaneous coupled rate equations. The present calculations for the reduced populations, as a function of electron densities, are plotted in Fig. 6 and Fig. 7 at two different electron temperatures for the Ar XVI ion.

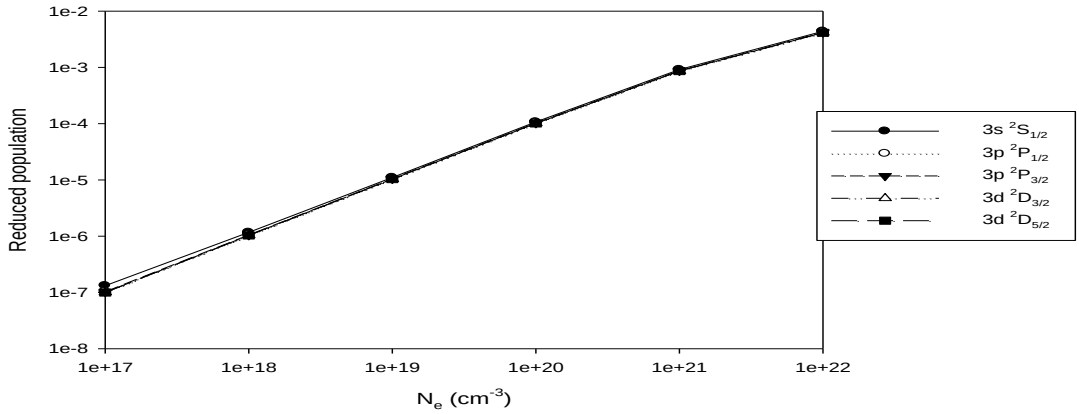

Fig. 6. Reduced population for selected levels of Ar XVI ion at the electron temperature equals to fourth the ionization potential.

Journal of. Modern Trends in Physics Research
Online ISSN 2636-4220
DOI: 10.19138/mtpr/(14)16-25
Accepted: 2014-12-19

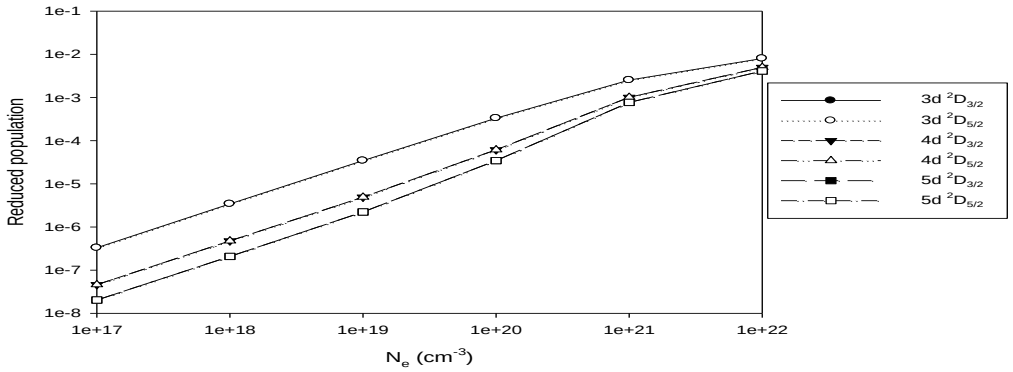

Fig. 7. Reduced population for selected levels of Ar XVI ion at the electron temperature equals to half the ionization potential.

The behavior of the level populations of the various levels of Ar XVI can be explained as follows: in general, at low electron densities the reduced population density is proportional to the electron density, where the collisional excitation rates increase with the electron densities and the collisional mixing of the excited levels may be ignored. This result is in agreement with those of Feldman and collaborators [Feldman, 1984; 1985;1986]. At high electron densities ($N_e \geq 10^{23}$ cm^{-3}), where the collisional excitation rates exceed the radiative decay rates, the reduced populations are independent of the electron density and are approximately equal for the levels having equal n.

3. Conclusion

The ionization and excitation rates have been calculated for 24 levels up to n = 5 in Ar XVI ion. Atomic data have been used to evaluate the rate coefficients and the reduced population densities for the ground and excited levels of Ar XVI. Simultaneous coupled rate equations for the 24 levels, under consideration, have been solved. At low electron densities, the population density is directly proportional to the electron density, where the excitation in the excited states is immediately followed by a radiative decay, and where the collisional mixing of the excited levels may be ignored. At high electron densities ($N_e \geq 10^{23}$ cm^{-3}), the radiative decay to all the levels will be negligible compared to the collisional depopulations and all the level populations become independent of electron density and are approximately equal. No data, theoretical or experimental, have been found in the literature for comparison.

Acknowledgements
I would like to thank Prof. Dr. Sami Allam, for his support.

REFERENCES

Allam, S. H. "CRMO-Collisional Radiative Model", computer code, private communication.

Cowan, R. D. (1981) *The theory of atomic structure and spectra*, University of California Press, Berkeley, California, pp. 214.

Cowan, R. D. and Griffin, D. C. (1976). Approximate relativistic corrections to atomic radial wave functions. *J. Opt. Soc. Am.*, **66**: 1010-1014.

Feldman, U., Bhatia, A. K. and Suckewer, S. J. (1983). Short wavelength laser calculations for electron pumping in Neon-Like Krypton (Kr XXVII). *App. Phys.*, **54**: 2188-2197.

Feldman, U., Seely, J. F. and Bhatia, A. K. (1984). Scaling of collisional pumped 3s-3p lasers in the Neon isoelectronic sequence. *J. App. Phys.*, **56**: 2475-2478.

Feldman, U., Seely, J. F. and Bhatia, A. K. (1985). Short wavelength laser calculations for electron pumping in Be I and B I isoelectronic sequences ($18 \leq Z \leq 36$). *J. App. Phys.*, **58**: 3954-3958.

Journal of. Modern Trends in Physics Research
Online ISSN 2636-4220
DOI: 10.19138/mtpr/(14)16-25
Accepted: 2014-12-19

Feldman, U., Seely, J. F., Doschek, G. A. and Bhatia, A. K. (1986). 3s–3p laser gain and X-Ray line ratios for the Carbon isoelectronic sequence. *J. Appl. Phys.*, **59**: 3953-3957.

Mu-Hong, Hu and Zhi-Wen, Wang (2009). Oscillator strengths for 2^2S--n^2P transitions of the lithium isoelectronic sequence from *Z = 11* to 20. *Chinese Phys.B* **, 18**: 2244-2249.

Nahar, S. N. (2002). Relativistic fine structure oscillator strengths for Li-like ions: C IV - Si XII, S XIV, Ar XVI, Ca XVIII, Ti XX, Cr XXII and Ni XXVI. A & A, **389**: 716-728.

Natarajan, L. and Natarajan, A. (2007). Effects of configuration interaction on the radiative rates of Li- and Be-like ions. *Phys. Rev.A*, **75**: 062502.

Seaton, M. J. (1987). Atomic data for opacity calculations. I. General description. *J. Phys. B: At. Mol. Phys.*, **20**: 6363-6378.

Safronova, U. I. and Shlyaptseva, A. S. (1996). Inner-shell excitation energy and autoionization rates for Li-, Be-, B-Like ions with Z = 6-54. *Phys. Scr.*, **54**: 254-270.

Safronova, U. I., Safronova, A. S. and Johnson, W. R. (2010). Relativistic many-body calculations of dielectronic satellite spectra created by autoionizing 1s2*l*2*l*' states in Li-like ions. *J. Phys. B: At. Mol. Opt. Phys.*, **43:** 144001.

Safronova, U. I., Shlyaptseva, A. S. and Golovkin, I. E. (1997). New atomic data for autoionizing states of Li-like ions with high values of N. *Phys. Scr.*, **T73:** 50-52.

Saloman, E. B. (2010). Energy levels and observed spectral lines of ionized argon, Ar II through Ar XVIII. *J. Phys. Chem. Ref. Data*, **39**: 033101.

Sapirstein, J. and Cheng, K. T. S-matrix calculations of energy levels of the Lithium isoelectronic sequence. (2011). *Phys. Rev.A*, **83**: 012504.

Stancalie, V., Pais, V., Mihailescu, A. and Chelmus, A.R.D. (2005). 32nd EPS Conference on Plasma Phys. Tarragona, 27 June - 1 July 2005 ECA Vol. **29C**, P-4.156.

Vriens**,** L. (1980). Cross sections for electron-impact ionization, excitation, deexcitation and total depopulation of excited atoms. *Phys. Rev. A.*, **22**:940-951.